Available online at www.sciencedirect.com
ScienceDirect
International Journal of Heat and Mass Transfer 50 (2007) 2582–2589
International Journal of HEAT and MASS TRANSFER
www.elsevier.com/locate/ijhmt

Laminar free convection underneath a downward facing inclined hot fin array

G. Mittelman, A. Dayan, K. Dado-Turjeman, A. Ullmann *

School of Mechanical Engineering, Tel Aviv University, Ramat Aviv, 69978 Tel Aviv, Israel

Received 18 July 2006; received in revised form 25 November 2006
Available online 9 March 2007

Abstract

A combined theoretical, experimental and numerical study was conducted to investigate the problem of laminar free convection underneath a hot isothermal and inclined fin array. The influence of inclination on the location where the flow stagnates, and splits, was examined. Heat transfer rates were calculated for different fin array geometries and temperatures. The results show that for small inclination angles the cooling rate is essentially constant. Beyond a certain angle, the tilting of the fin array enhances substantially the heat transfer rate. Sensitivity analyses indicate that the heat transfer coefficient increases at higher fin temperatures and larger fin spacing, but is of a lesser sensitivity to fin height changes. Additionally, it was discovered that the array optimal fin spacing do not depend on the inclination angle. In the theoretical part, a semi empirical model was developed for the heat transfer coefficient of horizontal and slightly inclined arrays that have large fin spacing. In effect it constitutes the necessary modeling addition to the previously developed model for moderately and tightly spaced fins of slightly tilted arrays. Together, they provide analytical expressions for the heat transfer coefficient of slightly inclined arrays, for any fin spacing.

Keywords: Fin; Fin array; Inclined; Free convection; Numerical; Experimental

1. Introduction

An investigation of the laminar free convection underneath a hot isothermal and inclined fin array is presented. A downward facing fin array is not the preferred orientation for effective cooling by natural convection. However, the architectural design requirements of modern telecommunication equipment give preference specifically to such hidden cooling devices. Therefore the exploration of this subject has begun only recently [1]. Horizontal downward facing fin arrays are of limited cooling capability. However, the tilting of the arrays substantially improves their cooling capacity, as demonstrated in the current investigation.

A literature survey has not unveiled any work on the subject of tilted downward facing fin arrays. In contrast, the subject of free convection underneath inclined hot isothermal flat strips has received considerable attention [2]. The latter exhibits convective heat transfer characteristics that apply to finned cooling surfaces as well. For inclination angles below 15° (roughly), it has been demonstrated that the ambient airflow that rises from below splits along a stagnation line, which is in between the center and the lower edge of the plate. The position of that line depends solely on the inclination angle and temperature difference. The exploration of the stagnation-line location for a flat surface is quite complex, and for a finned array seems to be even more complex. There it depends on the fin height and spacing. Tracking the location of the stagnation line is important since it defines the two array zones along which the convective flow moves in opposite directions, while affecting the heat transfer rate accordingly. Even the visualization of the flow is an extremely complicated

* Corresponding author. Tel.: +972 3 6407829.
E-mail address: Ullmann@eng.tau.ac.il (A. Ullmann).

0017-9310/$ - see front matter © 2007 Elsevier Ltd. All rights reserved.
doi:10.1016/j.ijheatmasstransfer.2006.11.033

Nomenclature

a	half the space between fins, m
C	boundary extension length (Fig. 3)
C_1, C_2	coefficients, Eq. (14)
F	correction factor
g	gravitational acceleration, m/s^2
h	local heat transfer coefficient, W/m^2 K
$\bar{h}$	average heat transfer coefficient, W/m^2 K
H	fin height, m
L	array half length, m
k	thermal conductivity, W/m K
$\dot{m}$	mass flux, kg/s m^3
$\overline{Nu}_L$	average Nusselt number, $\bar{h}L/k$
P	pressure
Pr	Prandtl number, v/α
Ra_L	Rayleigh number, $g\beta L^3\theta_w/\alpha v$
t	half the fin thickness, m
T	temperature, °C
v	horizontal velocity, m/s
V	characteristic velocity
w	vertical velocity, m/s
x	coordinate, m
y	coordinate, m
y^*	domain boundary, m
z	coordinate, m
z^*	domain boundary, m

Greek symbols

α	thermal diffusivity, m^2/s
β	thermal expansion coefficient, K^{-1}
δ	boundary layer thickness, m
v	kinematic viscosity, m^2/s
ϕ	inclination angle, deg
ρ	density
θ	temperature difference ($T - T_\infty$), °C

Subscripts

b	base
c	critical
eff	effective
H	horizontal
v	vertical
w	wall conditions
∞	ambient conditions

Superscript

s	strip

task since it is impossible to obtain a side view of the flow between the fins. Therefore, in the present investigation, the location of the stagnation line is tracked by numerical simulation. The present study is focused on exploration of the flow characteristics and their effects on the heat transfer rate, subject to the inclination angle.

Of special significance is the case of horizontal hot fin array facing down, which represents a limiting case of zero inclination angle. In the horizontal configuration, the convective boundary layer outer surface, excluding the array edge areas, can be either entirely outside or partially outside the array channels. The former case was previously investigated and its heat transfer coefficient was correlated according to [1]

$$\overline{Nu}_L = \frac{\overline{Nu}_L^s}{1+\frac{H}{a}}\left[\exp\left(-\frac{H}{2a}\right)+0.65\left(\frac{H}{a}\right)\left(\frac{L}{a}\right)^{-\frac{4}{5}}Ra_L^{\frac{1}{5}}\right]; \quad \phi = 0^\circ \tag{1}$$

where $\overline{Nu}_L$ is the averaged Nusselt number, $\overline{Nu}_L^s$ is the averaged Nusselt number for the horizontal infinite flat strip [3], Ra_L is the Rayleigh number, H the fin height, and a is the half fin spacing.

To complete the horizontal configuration modeling, a simplified expression for the case of partially filled channel (boundary layer confined within the channels) is also presented here. By definition, this case is of practical importance mainly for largely spaced fin arrays with high temperature differences.

2. Partially filled channel model

For free convection underneath hot surfaces, the boundary layer thickness δ is defined as the distance from the surface whereupon the airflow reverses its lateral movement direction and flows towards the surface edges [1]. When the boundary layer thickness is smaller than the fin height (Fig. 1a), the total heat transfer rate from the channel walls can be obtained by summing the heat fluxes from the horizontal and vertical plates:

$$(a+H)\theta_w h = (a+F\delta)\theta_w h_H + (H-F\delta)\theta_w \bar{h}_v \tag{2}$$

where h_H is the local heat transfer coefficient of the horizontal plate, $\bar{h}_v$ is the average heat transfer coefficient of

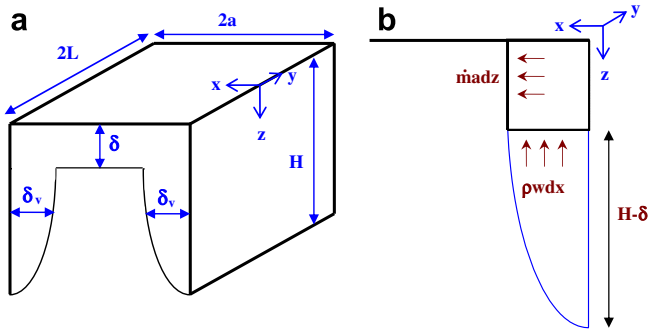

Fig. 1. (a) Boundary layers for the partially filled channel. (b) Mass conservation at the channel corner.

a vertical plate, h is the average local heat transfer coefficient on the channel cross section contour, δ is the local boundary layer thickness of the horizontal plate, and θ_w is the temperature difference between the channel surfaces and the surroundings (assumed to be constant).

The unknown contributions of the vertical and horizontal plates to the heat transfer rate from the channel corners are represented by the correction factor, F, which is determined empirically. This factor should also account for thermal and frictional effects imposed by the vertical fins (F turned out to be equal to 0.85). Since both of the solutions for the vertical and horizontal plates are known [4], it is only required to evaluate the local horizontal boundary layer thickness, δ, in order to calculate the channel heat transfer coefficient directly from Eq. (2). To evaluate δ, the horizontal flow is considered to be a flow underneath a flat plate (without fins) with a uniformly (along x) distributed mass source term $\dot{m}$ that accounts for the upward incoming flow from the vertical fins. The uniform source distribution is a consequence of the assumption that the horizontal flow would have a nearly uniform thickness in the x direction, i.e. $\delta \cong \delta(y)$ only. The corresponding volumetric mass flux (kg/m^3 s) is obtained from a simple mass balance at a channel corner (Fig. 1b):

$$\dot{m}a\,\mathrm{d}z\,\mathrm{d}y = \rho w|_{z=H-\delta}\mathrm{d}x\,\mathrm{d}y \tag{3}$$

ρ is the fluid density and w is the vertical velocity. Assuming that the vertical flow penetrates the horizontal flow through smooth stream lines, and based on the assumption that the vertical and horizontal profiles are similar, the relationship $\frac{\mathrm{d}x}{\delta_v|_{z=H-\delta}} \cong \frac{\mathrm{d}z}{\delta}$ must hold to satisfy continuity. The volumetric mass flux is given by: $\dot{m} \cong \frac{\rho w|_{z=H-\delta}}{a}\frac{\delta_v|_{z=H-\delta}}{\delta}$. Evidently, the mass-flux addition increases the horizontal boundary layer thickness.

The horizontal boundary layer thickness, δ, is obtained from the solution of governing equations of the two dimensional flow underneath flat plate with an added mass-flux source term.

The governing equations are based on the assumption of constant fluid properties (subject to the Boussinesq approximation), uniform fin array temperature and negligible thermal energy gain from mechanical dissipation. As for the Boussinesq assumption, previous investigation of similar problems [1,3] have reasonably justified its applicability even for relatively large temperature differences ($\theta_w <$ 80°C). Based on the aforementioned assumptions, the two dimensional conservation equations for laminar flow underneath a flat horizontal plate [3], including the mass, momentum and energy flux source terms (in bold letters) are

$$\rho\left(\frac{\partial v}{\partial y}+\frac{\partial w}{\partial z}\right) = \dot{\mathbf{m}} \tag{4}$$

$$v\frac{\partial v}{\partial y}+w\frac{\partial v}{\partial z}+\frac{\mathbf{v}\dot{\mathbf{m}}}{\boldsymbol{\rho}} = -\frac{1}{\rho}\frac{\partial P}{\partial y}+\nu\frac{\partial^2 v}{\partial z^2} \tag{5}$$

$$0 = -\frac{1}{\rho}\frac{\partial P}{\partial z}+g \tag{6}$$

$$\frac{\partial(vT)}{\partial y}+\frac{\partial(wT)}{\partial z} = \alpha\frac{\partial^2 T}{\partial z^2}+\frac{\dot{\mathbf{m}}}{\boldsymbol{\rho}}\mathbf{T}_v \tag{7}$$

where T_v is the upward flow temperature.

The boundary conditions are

$$\begin{aligned} &z=0, \quad v=w=0, \quad \theta=\theta_w \\ &z=\delta, \quad v=w=0, \quad \theta=0, \quad \frac{\partial v}{\partial z}=\frac{\partial\theta}{\partial z}=0 \\ &\text{and at} \quad y=0 \;\; v(z)=0 \end{aligned} \tag{8}$$

where θ is the temperature difference $(T-T_\infty)$. The density dependence on temperature, for the buoyancy force calculations of Eq. (6), is described by

$$\rho \cong \rho_\infty(1-\beta\theta) \tag{9}$$

where ρ_∞ is the surrounding fluid density and β is the thermal expansion coefficient which is $\beta \cong \frac{1}{T}$ for air.

Integrating Eq. (6) with the approximation of (9) yields

$$P = P_\infty - \int_z^\infty \rho_\infty g(1-\beta\theta)\,\mathrm{d}z \tag{10}$$

An additional boundary condition can be obtained at the surface $z=0$, where the first three terms of Eq. (5) vanish, since $v=w=0$. Combining Eqs. (5) and (10), and integrating from $z=0$ and $z=\delta$, yields

$$z=0, \quad \frac{\partial^2 v}{\partial z^2} = \frac{g\beta\theta_w}{3\nu}\frac{\partial\delta}{\partial y} \tag{11}$$

Based on the similarity profiles assumption for the temperature and velocity and subject to the boundary conditions (8), the following velocity and temperature profiles are adopted:

$$\begin{aligned} &\frac{v}{V} = \frac{z}{\delta}\left(1-\frac{z}{\delta}\right)^2 \\ &\frac{T-T_\infty}{T_w-T_\infty} = \frac{\theta}{\theta_w} = \left(1-\frac{z}{\delta}\right)^2 \end{aligned} \tag{12}$$

where V is a characteristic velocity that depends only on y. Note that also δ depends on y only. The assumption of similarity of the temperature and velocity profiles (Eq. (12)) within the boundary layer was tested successfully by numerical simulations and experiments [3].

It is assumed that the similarity characteristics (Eq. (12)) hold also for the flow underneath finned arrays. As the temperature profile is the same in both the horizontal and vertical boundary layers, the temperature of the mass-flux source is equal to the local temperature of the fluid in the horizontal boundary layer: $T_v = T$.

The solutions for the vertical boundary layer thickness, velocity profile and temperature distribution are [5]

$$\delta_v = C_2\sqrt[4]{z}$$
$$w = C_1\sqrt{z}\frac{x}{\delta_v}\left(1-\frac{x}{\delta_v}\right)^2 \qquad (13)$$
$$\frac{T-T_\infty}{T_w-T_\infty} = \left(1-\frac{x}{\delta_v}\right)^2$$

where the constants C_1, C_2 are

$$C_1 = 5.17\nu\left(\frac{20}{21}+\frac{\nu}{\alpha}\right)^{-\frac{1}{2}}\left(\frac{g\beta\theta_w}{\nu^2}\right)^{\frac{1}{2}}$$
$$C_2 = 3.93\nu\left(\frac{20}{21}+\frac{\nu}{\alpha}\right)^{\frac{1}{4}}\left(\frac{g\beta\theta_w}{\nu^2}\right)^{-\frac{1}{4}}\left(\frac{\nu}{\alpha}\right)^{-\frac{1}{2}} \qquad (14)$$

and α is the thermal diffusivity.

Based on the solution for the boundary layer thickness (Eq. (13)), the average heat transfer coefficient is calculated [5], and is

$$\bar{h}_v = \frac{4}{3}\frac{2k}{\delta_v|_{z=H-F\delta}} = \frac{8k}{3C_2\sqrt[4]{H-F\delta}} \qquad (15)$$

Likewise, the mass flux $\dot{m}$ can be estimated through the incorporation of Eq. (13):

$$\dot{m} = \frac{\rho w|_{z=H-\delta}}{a}\frac{\delta_v|_{z=H-\delta}}{\delta}$$
$$= \frac{\rho C_1 C_2}{a}(H_{\text{eff}}-\delta)^{(3/4)}\frac{z}{\delta^2}\left(1-\frac{z}{\delta}\right)^2 \qquad (16)$$

where H_{eff} is an effective fin height, corrected to include the fin tip heat transfer area: $H_{\text{eff}} = H + t$, where t is half of the fin thickness.

Substituting the velocity and temperature profiles (Eqs. (12)), along with the mass-flux term (Eq. (16)), into the conservation equations (4)–(7) and integrating across z from 0 to δ (based on the Leibniz's rule), yields a system of two ordinary, non-linear differential equations:

$$\frac{1}{105}\frac{d(V^2\delta)}{dy}+\frac{1}{6}g\beta\theta_w\delta\frac{d\delta}{dy}+\frac{\nu V}{\delta}=0$$
$$\frac{d(V\delta)}{dy} = \frac{60\alpha}{\delta}+\frac{C_1C_2}{a}(H_{\text{eff}}-\delta)^{\frac{3}{4}} \qquad (17)$$

With the boundary conditions:

$$y=0,\quad V=0$$
$$y=L,\quad \delta=\delta_c \qquad (18)$$

The term $\frac{C_1C_2}{a}(H_{\text{eff}}-\delta)^{\frac{3}{4}}$ represents the added mass flux emanating from the vertical flow. The boundary layer thickness at the channel edge, δ_c, is calculated for critical flow conditions underneath a flat plate [3]:

$$\delta_c = \left(\frac{2700\alpha^2L^2}{11g\beta\theta_w}\right)^{1/5} \qquad (19)$$

Assuming that the effect of added mass flux on δ_c at the channel edge is negligible, the solution (19) was incorporated in the finned array model.

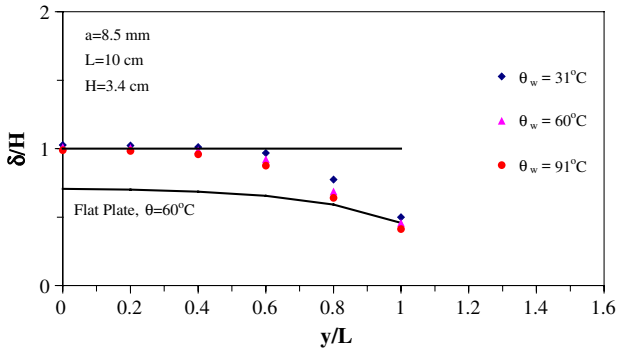

Fig. 2. Local boundary layer thicknesses for a flat plate and partially filled channel.

Eqs. (17), subject to the boundary conditions (18), are solved numerically for the unknowns: $\delta(y)$, $V(y)$. The overall channel heat transfer coefficient, h, is derived from the substitution of the "horizontal" heat transfer coefficient ($h_H = \frac{2k}{\delta}$) [4] and the "vertical" heat transfer coefficient (Eq. (15)) into Eq. (2), which yields

$$h = \frac{2k}{(a+H)}\left[\frac{a+F\delta}{\delta}+\frac{4(H-F\delta)^{3/4}}{3C_2}\right] \qquad (20)$$

To demonstrate the effect of the vertical flow mass influx into the horizontal flow, the local thickness boundary layer, $\delta(y)$, was calculated for a specific array geometry and various temperature differences (θ_w); and then it was compared to that of a flat plate for $\theta_w = 60\ ^\circ\text{C}$. The results are presented in Fig. 2. As seen, the fins produce a flow that increases the boundary layer thickness δ, which in turn reduces the horizontal surface heat transfer coefficient. As expected, the maximum boundary layer thickness is located at the array center line ($y = 0$). Reduction of the temperature difference tends to increase δ, up to a low threshold of $\theta_w = 30\ ^\circ\text{C}$, at which δ begins to exceed the fin height. That threshold also represents the validity limit of the partially filled channel model.

3. Experimental apparatus

Tests were conducted with an apparatus consisting of an insulated aluminum fin array that was electrically heated on its upper surface, as shown in Fig. 3. To evaluate the convective heat transfer rate, radiative heat fluxes from the fines and the heat losses through the insulation were calculated and subtracted from the input power. To evaluate the convective heat transfer rate, radiative heat fluxes and heat losses through the insulation were, both calculated and deducted from the input power. Thermal radiation losses were evaluated based on pertinent geometrical view factors and standard radiative network computations [6]. Surface emissivities were 0.87 and 0.95, according to each of the two coatings used. The experimental average heat transfer coefficient was obtained from the division of the convective heat transfer rate by, both, the total surface

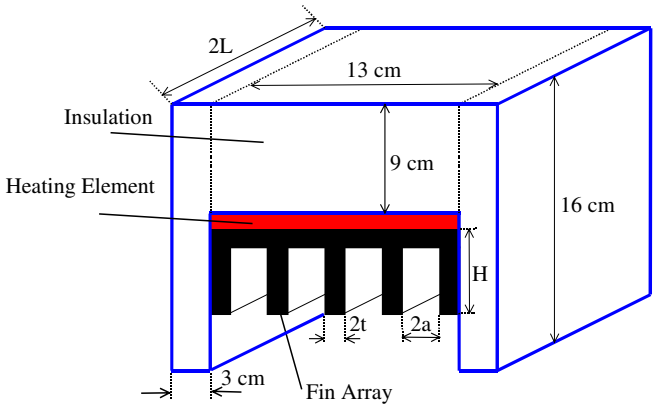

Fig. 3. Experimental setup.

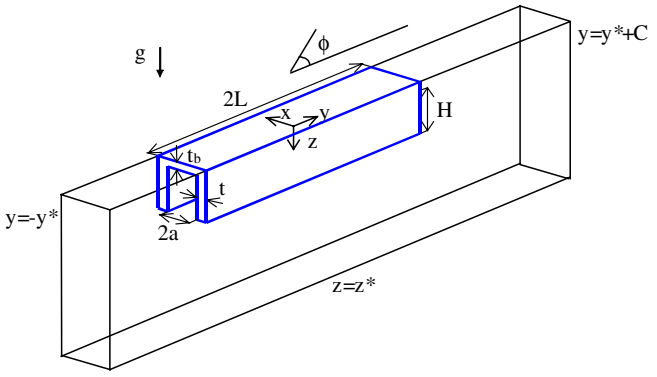

Fig. 4. Control volume for the numerical simulation of the inclined hot finned surface, facing down.

Table 1
Geometrical fin array dimensions for the investigated cases

	Case			
	1	2	3	4
$2t$ (mm)	2.2	2.2	2.2	2.2
$2L$ (cm)	20	20	20	20
H (cm)	2.15	2.15	3.4	3.4
$2a$ (mm)	7	17	7	17
Experimental	+	–	+	+
Numerical	+	+	+	+

fin array area and the surface to ambient temperature difference. Accuracy of the experimental heat transfer coefficient is smaller than 10% [7].

The test setup was assembled in a way that the inclination angle could easily be changed without interruption of the flow around the fin array. The test apparatus reliability was demonstrated through the successful reproduction of published experimental data for the heat transport underneath flat strips [1].

Three different fin arrays were tested; their dimensions are listed in Table 1. The tests were conducted for inclination angles ranging from 0° (horizontal case) to 30° and fins' temperatures within the range of 10–90 °C. A more detailed description of the experimental assembly was previously published [1,7]. The error of the experimental heat transfer coefficient is smaller than 10% of the reported data [7].

4. Numerical simulations

A numerical solution was conducted with the IcePak CFD software [8]. Illustration of the domain used for the numerical simulation is presented in Fig. 4. The gravity vector has two components: $g_y = g\sin\phi$, $g_z = g\cos\phi$. Being a tilted array, the flow underneath is asymmetrical in the y direction and therefore, in contrast to the horizontal case [1], the domain boundaries are not symmetrical. The adequate characteristic dimensions were found to be $y^* = 1.4L$, $z^* = 2L$, and $C = 0.4L$. Further extension of those dimensions does not produce any noticeable difference in the calculated heat transfer coefficient. The mesh size has been selected so as to be denser near the solid walls, to enhance the computation accuracies of the heat transfer coefficient and wall friction effects. To validate the numerical scheme computations, the grid size was continuously reduced up to a point were further reductions ceased to affect the results (changes smaller than 1%). A more detailed description of the numerical model was previously published [1]. The numerical solution was obtained for the four different fin array setups (Table 1).

5. Results and discussion

The partially filled channel model was tested against experimental data of horizontal fin arrays. The results are presented in Fig. 5. As aforementioned, the model is applicable only for temperature differences which satisfy the condition of partially filled channels ($\delta < H$). As seen, the model successfully reproduces the dependence trend of the measured heat transfer coefficient on temperature, but is somewhat over predictive.

The flow streamlines underneath horizontal and inclined fin arrays were calculated by the numerical model. As indicated in Fig. 6a, the streamlines underneath a horizontal array are symmetrical and the stagnation line (flow separa-

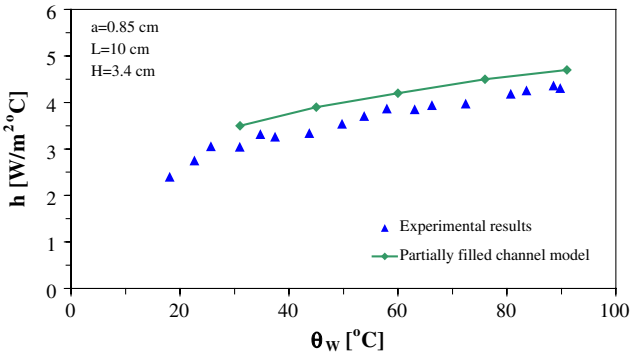

Fig. 5. A comparison between the partially filled channel model and experimental data of heat transfer coefficients for horizontal fin array.

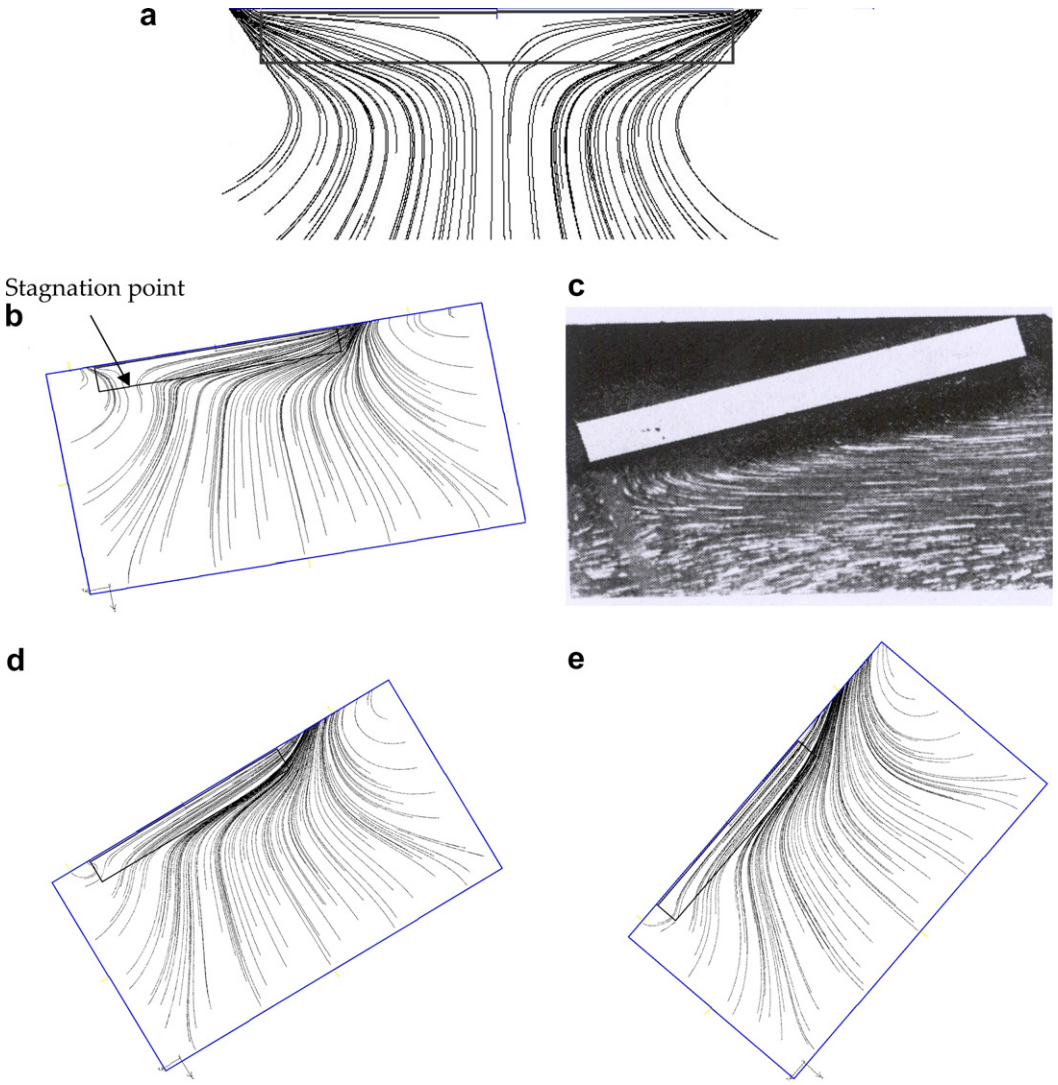

Fig. 6. Streamlines underneath heated arrays ($H = 2.15$ cm) for various inclination angles: (a) horizontal array, $\phi = 0$; (b) array with $\phi = 10.661°$, $\theta_w = 54.2$ °C; (c) plate [2], $\phi = 15°$; (d) array with $\phi = 30.997°$, $\theta_w = 47.5$ °C ; (e) array with $\phi = 44.0°$, $\theta_w = 44.0$ °C.

Table 2
Inclination angles in which the stagnation point is at the fin edge for different geometries and temperature differences $L = 10$ cm

$2a$ (mm)	H (cm)	θ_w (°C)	ϕ (deg)
17	2.15	56	8
17	3.4	56	10
17	3.4	24.5	15
7	3.4	56	20

tion) is located at the array center [1]. Increasing the inclination angles (Fig. 6b, d and e) moves the stagnation line towards the lower edge of the fin. That phenomenon was also experimentally observed in the case of flat strip, as shown in Fig. 6c [2], whereupon the flow separates at the plate edge. The rectangular contours in Fig. 6 represent the boundaries of the numerical computation domain.

Calculated minimal inclination angles at which the stagnation lines reach the fin arrays edge are listed in Table 2 for various conditions. Higher sensitivity of the stagnation-line position to the inclination angle is associated with larger fin spacing, higher temperature difference and smaller fin height. Larger fin spacing (less friction) and higher temperature difference (driving force) enhances the inertia of the fluid that flows to the left side of the array (Fig. 6b) hence resisting the movement of the flow separation line towards the array edge. A larger fin height simultaneously increases the driving force and increases friction, thus producing mutually offsetting effects and thereby reducing sensitivity.

To validate the numerical model, a comparison between the numerical simulations and experimental data was carried out and plotted in Fig. 7. The results represent a complete set of experiments conducted with different array geometries, inclination angles (including zero) and temperature differences. As seen, the numerical predictions and the experimental data are in good agreement. The numerical simulation over predicts the heat transfer coefficients at higher array inclination angles (which is associated with

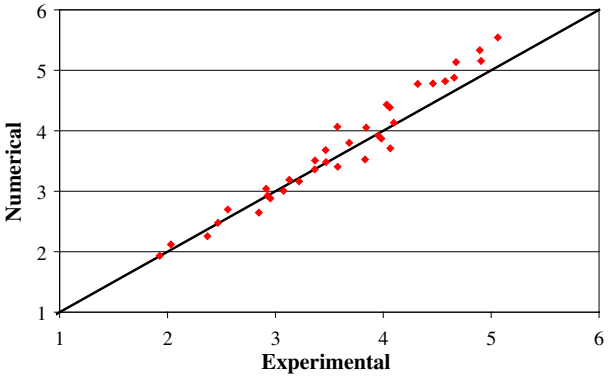

Fig. 7. A comparison between experimental and numerical heat transfer coefficients (W/m^2 K).

higher heat transfer rates). This deviation can be attributed to the inadequacy of the experimental setup for large inclinations testing, being originally designed for horizontal and moderately inclined fin arrays.

Experimental and numerical calculations of the heat transfer coefficients as a function of inclination angle and temperature difference for a specific geometry (case 4 – Table 1) are depicted in Figs. 8 and 9. As indicated by the error bars, the experimental and numerical data are in an agreement of ±12%. Expectedly, owing to stronger buoyant forces, larger heat transfer coefficients are obtained at higher array surface temperatures and steeper inclination angles. Furthermore, the heat transfer is more sensitive to the inclination when the stagnation-line position moves towards the fin array edge (roughly $\phi = 10$–$20°$ – region 2). Inclination angle effects on the heat transfer coefficient are small at low angles (0–10° – region 1). Apparently, for these angles, the heat transfer coefficient can simply be calculated by either Eq. (1) or (20), depending if the boundary layer exceeds the channel depth or not, respectively. In Fig. 9, the well known solution of vertical (90° inclination) fin array (Van De Pol correlation [9]) is drawn too. The values of those points clearly imply that

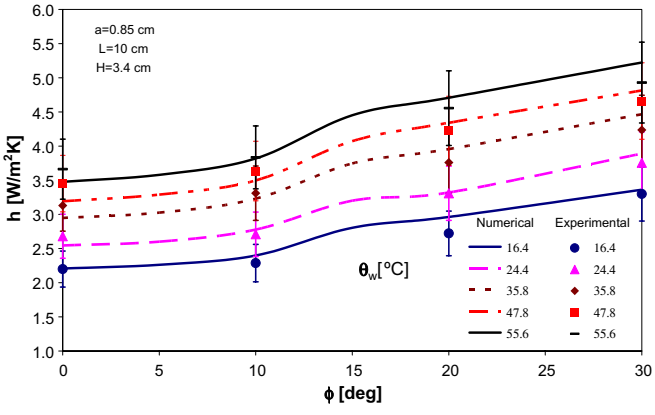

Fig. 8. The dependence of the heat transfer coefficient on the inclination angle and temperature difference for $L = 10$ cm, $H = 3.4$ cm and $a = 8.5$ mm.

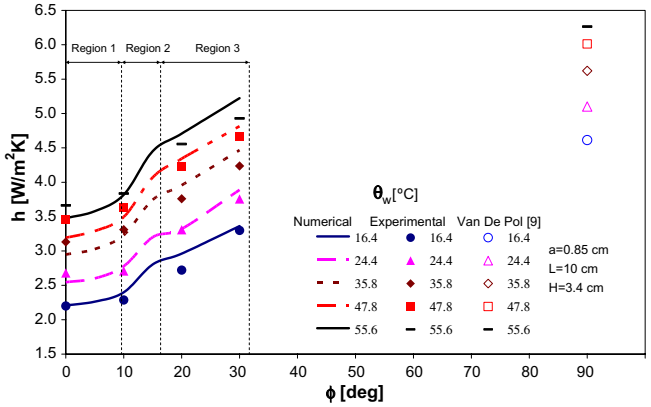

Fig. 9. The dependence of the heat transfer coefficient on the inclination angle and temperature difference for $L = 10$ cm, $H = 3.4$ cm and $a = 8.5$ mm. The solution of vertical fin array [9] is also shown.

the heat transfer enhancement owing to inclination extends up to inclination of 90° (region 3).

A modified Van De Pol correlation, obtained through the replacement of g by $g\sin\phi$, is presented in Fig. 10. Clearly, the modified formula cannot track the actual effect of array inclination on the heat transfer rate. Furthermore, the modified formula does not account for the stagnation-line location. This probably explains the large disagreement of results at small inclination angles.

The numerical model was further used to explore the direct influence of the fin array geometry on the cooling rate. The effect of the fin height is presented in Fig. 11 for various temperature differences. Similar to horizontal arrays [1,7], the effect of fin height on the heat transfer coefficient in inclined arrays is relatively small. This stems from the fact that up to a certain height the increase of the fin heights does not enhance the buoyant force but increases the drag force, and thus reduces the averaged heat transfer coefficient. Beyond that height, there are mutually offsetting effects of gains in, both, the buoyancy force and drag. Nonetheless, being the driving force, the buoyancy gain of longer fins is slightly more influencing, and therefore enhances the heat transfer coefficient.

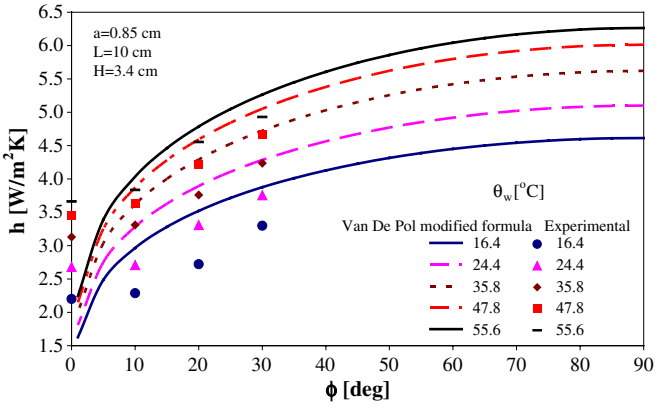

Fig. 10. Comparison between experimental results and Van De Pol [9] modified formula for $L = 10$ cm, $H = 3.4$ cm and $a = 8.5$ mm.

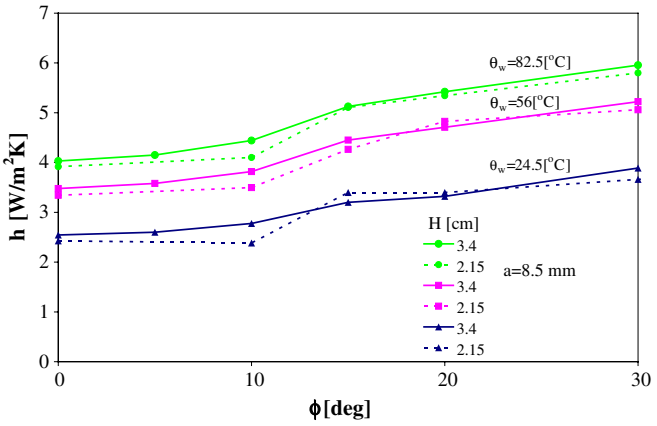

Fig. 11. The influence of the fin height on the heat transfer coefficient at different inclination angles and temperature differences.

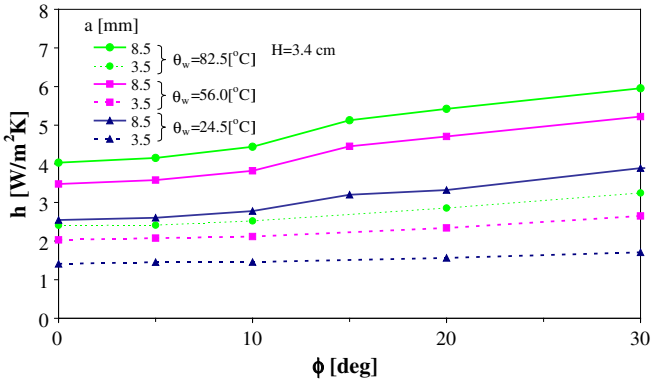

Fig. 12. The influence of the fin spacing on the heat transfer coefficient at different inclination angles and temperature differences.

As seen from Table 2, the smaller the fin spacing, the lower is the sensitivity of the stagnation-line location to the inclination angle. This could also be observed in Fig. 12 for arrays with 3.5 mm fin spacing. Larger fin spacing, in effect, reduces drag and thereby increases the heat transfer coefficient. However, for a specified base area of an array, increasing the fin spacing reduces the total cooling surface area. This adverse influence of large fin spacing on the heat transfer rate per unit base area was previously discussed for the case of horizontal array [1]. In the latter, a way to determine the optimal fin spacing was suggested. Apparently, the optimal spacing for horizontal arrays [1] is also applicable for inclined arrays with inclination angles above 20°. In these angles, the variation of the heat transfer coefficient with inclination (the slope of the lines in Fig. 12) is weakly dependent on the fin spacing.

6. Conclusions

A combined numerical and experimental investigation on the free convection underneath inclined hot fin arrays was conducted. In addition, a semi empirical model for fin arrays with large fin spacing and high temperature difference (partially filled channels) was developed and calibrated successfully against experimental data. A good agreement between the numerical and experimental heat transfer rates was obtained. The effects of the inclination angle, temperature difference and fin array geometry on, both, the location of the flow stagnation line and heat transfer rate were demonstrated. To conclude:

- Similarly to the flat strip case, the stagnation-line location reaches the lower edge of the arrays at inclination angles as small as 15°.
- The heat transfer rate is substantially larger when there is no flow separation along the fin array. Therefore, it is advised to tilt the array to angles greater than 10°.
- The heat transfer coefficient increases at higher temperature differences and larger fin spacing, but is slightly dependent on the fin height.
- The optimal fin spacing of tilted arrays is almost identical to that of horizontal arrays.

References

[1] A. Dayan, R. Kushnir, G. Mittelman, A. Ullmann, Laminar free convection underneath a down facing hot finned array, Int J Heat Mass Transfer 47 (2004) 2849–2860.
[2] T. Fujii, H. Imura, Natural-convection heat transfer from a plate with arbitrary inclination, Int J Heat Mass Transfer 15 (1972) 755–767.
[3] A. Dayan, R. Kushnir, A. Ullmann, Laminar free convection underneath a hot horizontal infinite flat strip, Int J Heat Mass Transfer 45 (2002) 4021–4031.
[4] A. Bejan, Convection Heat Transfer, Wiley and Sons Inc., New York, NY, 1995.
[5] E.R.G. Eckert, E. Soehngen, Studies in heat transfer, US Air Force Technical Report 5747, December 1948.
[6] B. Abramzon, A simple closed-form solution for evaluation of radiative heat transfer from a rectangular fin array, IEEE Trans. Compon. Pack. Manuf. Technol. – Part A 20 (2) (1997) 225–229.
[7] G. Mittelman, Experimental study of free convection from a hot finned array, M.Sc. Thesis, Tel Aviv University, 2001.
[8] Icepak 4 User's Guide, Fluent Inc., 2003.
[9] A.D. Kraus, A. Aziz, J. Welty, Extended Surface Heat Transfer, Wiley and Sons Inc., New York, NY, 2001.